International Journal of Science and Research (IJSR)
ISSN: 2319-7064
SJIF (2022): 7.942

Analysis of Proton Radiotherapy Dose Distribution in Pediatric Medulloblastoma Cases Using MCNP 6.2.0

Sulvy Rahmawati[1], Eko Hidayanto[2], Fajar Arianto[3]

[1, 2, 3]Department of Physics, Faculty of Science and Mathematics, Diponegoro University, Semarang, Indonesia
[2]Corresponding Author Email: *ekohidayanto[at]gmail.com*

Abstract: ***Proton radiotherapy is a new modality that has the potential to treat tumors to therapeutic levels. Proton sources are superior to photons for radiotherapy because the maximum dose is distributed over the tumor target and minimally affects healthy tissue. Proton radiotherapy has the potential to be used in pediatric tumor cases, one of which is in the treatment of medulloblastoma in children aged 10 years. The use of clinical proton radiotherapy is still very small, so treatment planning in this study used the Monte Carlo simulation method. This research was conducted to determine the target dose distribution to the tumor and healthy tissue around the cancer. This research uses the Monte Carlo N – Particle (MCNP) 6.2.0 program to run the simulation. The proton radiotherapy simulation uses a benchmarking nozzle from previous research taken from the Nozzle Everything Upstream (NEU) program, as well as using a 10 - year - old whole - body Oak Ridge National Laboratory – Medical Internal Radiation Dose (ORNL – MIRD) phantom. The ORNL - MIRD phantom is illuminated by protons from the posterior direction and then the dose is calculated. The simulation dose calculation is set on the MCNP tally. The research results showed that the dose distribution in the Clinical Target Volume (CTV) was (19.82 ± 0.099) Gy RBE and the Planning Target Volume (PTV) was (18.07 ± 0.072) Gy RBE. In addition, the brain, skull and spinal cord as OAR received a relative dose percentage to the tumor of 4.64%, 1.58% and 0.0607% respectively. In this study, proton radiotherapy in the treatment of brain tumors was get the dose distribution to therapeutic levels.***

Keywords: Proton radiotherapy, pediatric medulloblastoma, MCNP 6.2.0

1. Introduction

Brain cancer is one of the cancer cases with a fairly high death rate. In 2020, there were 308, 102 new cases of brain and central nervous system tumors recorded worldwide with a death toll of 251, 329. In Indonesia, cases of brain and central nervous system tumors are ranked 15th based on the number of new cases in 2020, namely 5, 964 people and 5, 298 deaths [1]. Brain tumors are divided into benign and malignant brain tumors, with benign tumors including meningiomas, pituitary tumors, nerve sheath tumors, and neuroepithelial tumors. Malignant brain tumors or cancer include glioblastoma, meninges tumor, lymphoma, hemopoitic neoplasm, anaplastic astrocytoma, and medulloblastoma. One type of brain cancer that many pediatric patients suffer from is medulloblastoma. Medulloblastoma in children often appears between the ages of 1 and 10 years [2].

Treatment of medulloblastoma cases aged > 3 years is carried out by implementing extensive recession, followed by radiotherapy and chemotherapy [3]. Currently, radiotherapy using the photon modality has been widely used clinically. Photon technology applies dose limitation to healthy tissue using variations in radiation intensity. However, limiting the dose to healthy tissue can increase the treatment volume resulting in a larger patient integral dose. This raises concerns about the possible side health effects, especially in pediatric patients who are expected to have a higher life expectancy, thus triggering the potential for other more effective modalities, namely using protons.

Proton modality uses charged proton particles. When a proton hits a target, it quickly loses energy at the end of its path. Localized dose peaks can be generated into a graph called the Bragg peak which was discovered in the 1900s by William Bragg. The greater the initial energy of the proton, the deeper the Bragg peak graph will be. Proton radiotherapy is often an option in the treatment of pediatric patients because it can provide the potential for a longer life span, minimal radiation exposure, thereby avoiding long - term radiation risks [4]. The use of proton radiotherapy for two decades and to date, has more than 100 working proton surgery centers. However, less than 1% of the world's radiotherapy patients receive treatment using protons and heavy ions [5].

Proton radiotherapy treatment planning is carried out by creating a Treatment Planning System (TPS) including Planning Target Volume (PTV), Clinical Target Volume (CTV), and Gross Tumor Volume (GTV) as well as Organs at Risks (OARs) so that proton treatment can reach therapeutic levels [6]. Apart from that, planning particle and ion therapy also needs to pay attention to the Relative Biological Effectiveness (RBE) value generated [7]. However, the small number of proton surgery centers and limited access limit the potential clinical use of TPS so that it can be carried out using Monte Carlo - based simulations. Monte Carlo simulation is considered more accurate in calculating dose distribution [8]. In proton radiotherapy planning, various Monte Carlo based programs can be used, such as Geometry and Tracking (GEANT4), Particle and Heavy Ion Transport code System (PHITS), FLUKA, and Monte Carlo N - Particle (MCNP) [9]. The Monte Carlo N - Particle Program (MCNP) is a radiation transport code that aims to track particle types over a wide energy range. The MCNP program has the latest version released in 2018, namely MCNP 6.2.0 [10].

The Monte Carlo program has been proven to be able to be used in proton radiotherapy simulations. In the research of Rahmawati et al., (2022), a simulation of proton radiotherapy was carried out in lung cancer cases using the MCNP 6 program. In this study, treatment planning began with determining the isodose in the treatment area so that optimal dose distribution was obtained. Apart from that, in the research of Fianto et al., (2022), the PHITS 3.24 program was used to compare simulations of passive scattering and pencil beam proton radiotherapy in pediatric medulloblastoma cases. As a result, the passive scattering radiation technique produces a more homogeneous dose distribution in the cancer area. This research was conducted to analyze the distribution of radiation doses in medulloblastoma in children aged 10 years using proton passive scattering radiotherapy modality using the MCNP 6.2.0 program. Treatment planning in this study begins with determining the isodose percentage of 95 - 107% at the tumor depth [11].

2. Methods

This research uses software in the form of the MCNP 6.2.0 program, Total Commander, Visual Editor X_24E, and Notepad++ to carry out simulations as well as Microsoft Excel 2021 and Microsoft Word 2021 for data processing. The geometry data used in this simulation is divided into 2, namely phantom geometry and prototype nozzle. This study used the Oak Ridge National Laboratory - Medical Internal Radiation Dose (ORNL - MIRD) phantom geometry throughout the body of a 10 year old child. The target tumor is a case of medulloblastoma (M+) in the posterior fossa which is located in the back of the brain, close to the spinal cord. The dose planning given to the target tumor is posterior fossa boost treatment of 19.8 Gy RBE, with 1.8 Gy RBE for one fractionation in high risk (M+) cases [12]. Healthy tissue and tumors in the ORNL - MIRD phantom are composed of elemental mass fraction components according to the 2011 International Commission on Radiological Protection (ICRP) report [13]. The depiction of the tumor is spherical, consisting of a CTV with a radius of 1.5 cm and a PTV with a margin of 0.5 cm [14]. The organs taken into account in the simulation are PTV, CTV and Organ at Risks (OARs) target organs, including the skull, brain and spinal cord located around the cancer. The phantom geometry display can be seen in Figure 1.

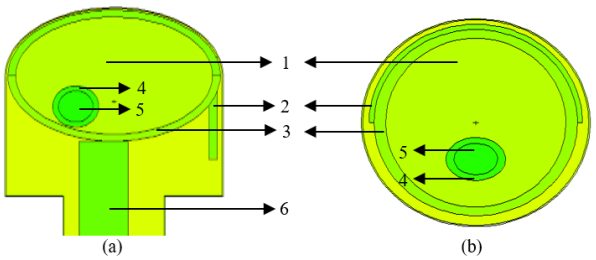

Figure caption: 1. Brain, 2. Facial skeleton, 3. Skull, 4. PTV, 5. CTV, 6. Spinal cord

Figure 1: ORNL - MIRD phantom view of the head (a) sagittal view (b) axial view

Proton nozzle geometry data using passive scattering benchmark nozzles from research by Jeffrey M. Ryckman (2011). The nozzle has been designed by taking various clinical data and Nozzle Everything Upstream (NEU) program data. The proton generator comes from a cyclotron designed using Ion Beam Applications (IBA). The current at the IBA nozzle is assumed to be 94 nA [15]. The proton beam in this nozzle design applies double scattering distributed in a Gaussian manner in the range - compensated scatterer. This double scattering produces a homogeneous proton beam output and can regulate the depth of dose penetration in tissue via the Range Modulation Wheel (RMW). The proton energy used in passive scattering radiation is around 225 MeV – 250 MeV. This is because the light is formed from a double scattering process, so it requires a fairly large energy input [8]. The nozzle specifications set out in this research and the nozzle geometry are presented in figure 2.

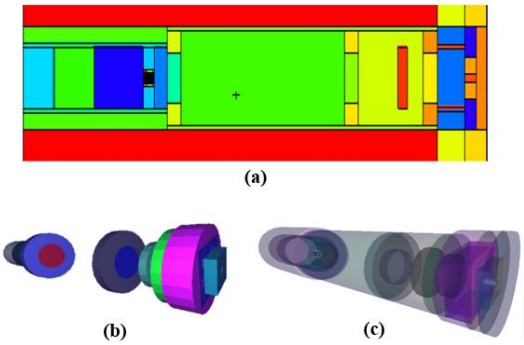

Figure 2: (a) nozzle geometry (b) nozzle in 2D (c) nozzle in 3D

This research uses simulation calculations to obtain the absorbed dose of protons which is measured in Gy and the dose of secondary neutron particles is calculated to be equivalent to the equivalent dose (Sv). Calculation of proton and neutron doses to tumor targets and OARs can use Fn tally. Proton dose calculations can use the F6 tally which functions to calculate the average energy in a cell in units of MeV/g/s/particle source, then converted into units of Gy/s/particle source [16]. In calculating the neutron dose, the neutron equivalent dose is obtained using tally F4 [17]. Based on the ICRP 92 report of 2003, the equivalent dose equation can be written in equation 1.

$$H_T = \sum_R W_R D_{T,R} \quad (1)$$

H_T is the equivalent dose (Sv), W_R is the radiation weight factor, $D_{T,R}$ is the average absorbed dose to tissues and organs (Gy) [18].

At the simulated output dose value, multiplication is carried out by the number of protons according to the size of the source current used. Determination of the number of protons in proton radiotherapy is written in equation 2.

$$I = \frac{\Sigma q}{t} \quad (2)$$

I is the reference current value of the source used (A), Σq is the number of proton particles flowing and t is the time required for protons to flow (s) [19]. In calculating the amount of simulated fractionation, based on the total planned dose, fractionation is obtained by dividing the planned dose by the perfraction dose. To calculate the amount of fractionation, can use equation 3 [20].

$$\text{Fractionation amount} = \frac{\text{Planned Dose (Gy RBE)}}{\text{Dose per fraction (1,8 Gy RBE)}} \quad (3)$$

3. Results and Discussion

Calculation of dose distribution to tumor cells begins by determining variations in energy combinations at the depth of the tumor. Energy variations are needed to see the quality of illumination on the target [19]. The energy range varied was 223 - 236 MeV, with the direction of radiation from the back of the head adjusting the position of the tumor. From the simulation results, the best energy combination at the depth of the tumor is selected. The results of several isodose curves with a combination of 3 energies can be seen in Figure 3.

The tumor depth modeled in this study was 4 - 8 cm below the skin counting from the PTV. The tumor area should receive the highest proton absorbed dose possible with healthy tissue receiving a low dose. The best results obtained from the isodose graph are seen in Figure 3 graph (a). The energy combination of 230, 233, and 236 MeV in graph (a) is able to provide the maximum absorbed dose for the entire PTV and CTV tumor area better than the other 3 combinations. Isodose charts also prove that the use of energy variations in proton radiotherapy greatly influences the treatment plan [21]. The planning dose for medulloblastoma (M+) in this research model received an additional dose in the posterior fossa of 19.8 Gy RBE and 1.8 Gy RBE for dose per fraction, with 11 times fractionation. In this study, the current is considered to have a value of 94 nA [15]. Furthermore, the tumor absorbed dose distribution value in the results of this study for CTV was (19.82 ± 0.099) Gy RBE and (18.07 ± 0.072) Gy RBE at PTV. This tumor dose distribution is in accordance with the ICRU 78 report of 2007, namely that the tumor received a dose of 95 - 107% of the planned dose [22].

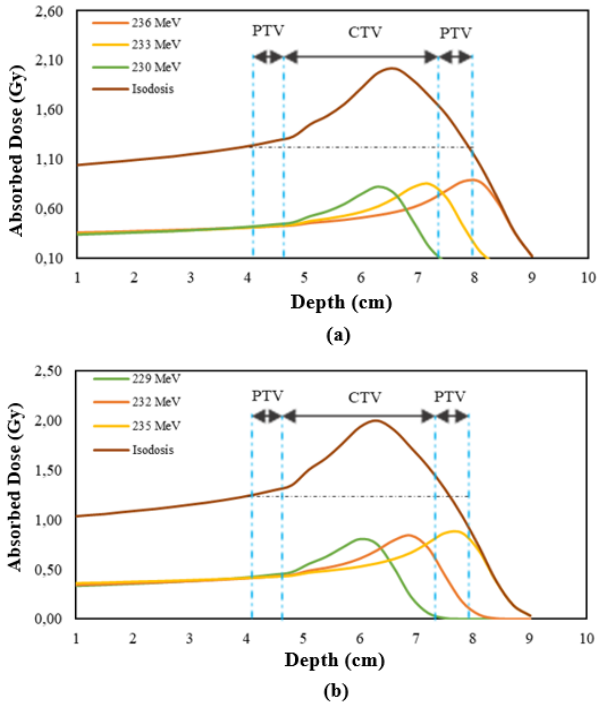

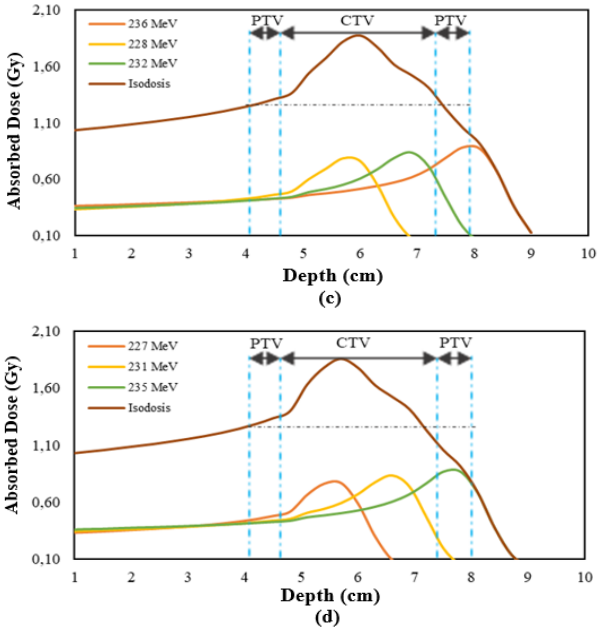

Figure 3: Isodose graph for each energy variation (a) energy variations 230, 233, and 236 MeV (b) energy variations 229, 232, and 235 MeV (c) energy variations 228, 232, and 236 MeV (d) energy variations 227, 231, and 235 MeV

Radiotherapy Organ at Risks (OARs) doses also need to be considered. The healthy organs taken into account in this study consisted of the brain, skull and spinal cord. The skin and eyes, which are also part of the OARs, were not taken into account in this study. This is due to the shape of the MIRD phantom throughout the body, making it difficult to identify the eye organs and special skin volumes in the head area. Simulation of all OARs was carried out using MCNP 6.2.0 with 15 million particles for approximately 7 hours.

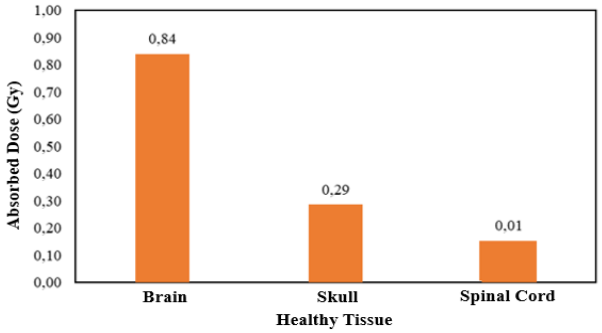

Figure 4: OAR dose distribution

The brain receives the highest absorbed dose compared to other organs. This is because the tumor is located in the brain and the brain is before the depth of the tumor so that when the proton beam passes, the brain area absorbs a lot of the dose. The dose distribution results obtained were then compared with the absorbed dose limits for each OAR based on Quantitative Analysis of Normal Tissue Effects in the Clinic (QUANTEC) data. The OAR dose limits are presented in table 2.

Table 1: OAR absorbed dose limit [23], [20]

Tissue	Maximum Dose (Gy RBE)
Brain	60
Spinal Cord	50
Skull	52

Based on the results obtained in graphic figure 4, the dose across the OAR received a very low distribution when compared with the maximum dose limit in table 1. In addition, comparisons were also made for the relative dose to tumor cells. The comparison results obtained are presented in table 2. Based on the comparison of the absorbed dose to the tumor, OARs still received a very low dose percentage compared to the standard dose percentage ≤ 75 - 90% [24], [25]. Apart from that, the comparison of OARs doses is also relevant to the research of Fianto et al. (2022), who examined dose distribution in cases of medulloblastoma in children aged 10 years using simulations on passive scattering proton radiotherapy. In all OARs, the dose received was still very low for cases of medulloblastoma in children aged 10 years. This proves that healthy organs around the tumor with proton radiotherapy treatment are still within very safe limits.

Table 2: Comparison of doses of OARs relative to tumor

Tissue	Standard	Relative to Tumor Cells	[12]
Brain	≤ 90 %	4.64 %	4.07%
Spinal Cord	≤ 78 %	1.58%	51.33%
Skull	≤ 75 %	0.0607%	2.24%

Proton radiotherapy is a promising modality because it can minimize toxicity by reducing radiation exposure to normal tissue compared to photon radiotherapy. Apart from that, proton radiotherapy can also maintain a good distribution of the dose to the target so that it can create a typical proton Bragg Peak curve [26]. After obtaining the dose distribution in proton radiotherapy, the dose was then compared to the 6 MV photon modality of the 3DCRT technique for medulloblastoma cases in the study of Helal et al. (2014) [27]. In this study, the tumor was irradiated using a Multi Leaf Collimator (MLC) to control the distribution of the light that came out. The results of comparing these two modalities can be seen in Figure 5.

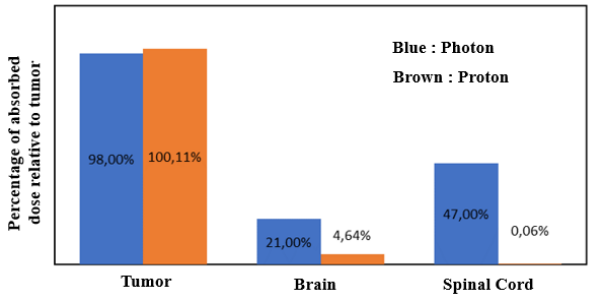

Figure 5: Comparison graph of protons and photons

Based on this graph, the OARs distribution value for proton radiotherapy is still much lower than for photon radiotherapy. This proves that proton radiotherapy is far superior in treating radiation exposure to healthy tissue, making it suitable for treating cases of pediatric patients. However, it should be remembered that proton radiotherapy can produce high LET neutron distribution with different energies for passive scattering and pencil beam radiation so that the use of the radiation system in proton radiotherapy needs to pay attention to the complexity of the tumor [28].

4. Conclusion

Based on research that has been carried out, it was concluded that determining energy depends on the position and depth of the tumor under the skin. The best energy obtained and used in this study was 230, 233, and 236 MeV based on planning with the tumor receiving 95 - 107% of the planned dose. Tumor cells have achieved a dose uptake of 100.11% of clinical planning. The dose distribution in the Clinical Target Volume (CTV) was (19.82 ± 0.099) Gy RBE and the Planning Target Volume (PTV) was (18.07 ± 0.072) Gy RBE. In addition, the brain, skull and spinal cord as OARs received a relative dose percentage to the tumor of 4.64%, 1.58% and 0.0607%, respectively. All OARs achieve a very low dose distribution within the maximum radiation limit and proton radiotherapy is proven to be superior to photon radiotherapy. .

References

[1] The Global Cancer Observatory. Cancer Incident in Indonesia. *Int. Agency Res. Cancer* **858**, 1–2 (2020).
[2] Miller, K. D. dkk. Brain and other central nervous system tumor statistics, 2021. *CA. Cancer J. Clin.7***1**, 381–406 (2021).
[3] Pollack, I. F., Agnihotri, S. & Broniscer, A. Childhood brain tumors: Current management, biological insights, and future directions. *J. Neurosurg. Pediatr.2***3**, 261–273 (2019).
[4] Oertli, D. B. Proton Dose Assessment To The Human Eye Using Monte Carlo N - Particle Transport Code (MCNPX). (2006).
[5] Mohan, R. A review of proton therapy – Current status and future directions. *Precis. Radiat. Oncol.6*, 164–176 (2022).
[6] Fahrurrozi, H., Harto, A. W., Triatmoko, I. M., Wijaya, G. S. & Sardjono, Y. Dose Optimization on Liver Cancer Proton Therapy and Boron Neutron Capture Therapy Using Particle and Heavy Ions Transport Code System. *J. Teknol. Reakt. Nukl. Tri Dasa Mega* **23**, 33 (2021).
[7] Loap, P. & Kirova, Y. Fast neutron therapy for breast cancer treatment: An effective technique sinking into oblivion. *International Journal of Particle Therapy* vol.7 61–64 (2021). Guan, F. Design and Simulation of A
[8] Passive - Scattering Nozzle in Proton Beam Radiotherapy. vol.73 (Tsinghua University, 2009).
[9] Hashemi, Z., Tatari, M. & Naik, H. Simulation of dose distribution and secondary particle production in proton therapy of brain tumor. *Reports Pract. Oncol. Radiother.2***5**, 927–933 (2020).
[10] C. J. Werner, dkk. *Mcnp 6. MCNP Version 6.2 Release Notes*. https: //permalink. lanl. gov/object/tr?what=info: lanl - repo/lareport/LA - UR - 18 - 20808 (2018).
[11] Rahmawati, F., Khairunnisa, A. F., Riyatun & Suharyana. Analysis of dose distribution in proton therapy for lung cancer with MCNP code. *J. Phys. Conf. Ser.2***190**, (2022).
[12] Fianto, M. M. D. dkk. Dose Distribution Analysis of Proton Therapy for Medulloblastoma Cancer With Phits 3.24. *J. Teknol. Reakt. Nukl. Tri Dasa Mega* **24**, 27 (2022).
[13] Hauswald, H. dkk. First experiences in treatment of low

- grade glioma grade I and II with proton therapy. *Radiat. Oncol.7*, 1–7 (2012).
[14] Min, C. H. dkk. Evaluation of permanent alopecia in pediatric medulloblastoma patients treated with proton radiation. *Radiat. Oncol.9*, 220 (2014).
[15] Ramadhan, M. Y. Analisis Dosis Pada Pengobatan Penyakit Kanker Otak Glioblastoma Multiforme Dengan Metode Boron Neutron Capture Therapy (BNCT) Menggunakan Particle And Heavy Ion Transport Code System (PHITS). (Universitas Negeri Yogyakarta, 2018).
[16] Hernandez, S. dkk. Resection cavity auto-contouring for patients with pediatric medulloblastoma using only CT information. *J. Appl. Clin. Med. Phys.* (2023) doi: 10.1002/acm2.13956.
[17] Ryckman, J. M. Using Mcnpx To Calculate Primary and Secondary Dose in Proton Therapy. (Georgia Institute of Technolog, 2011).
[18] Pidikiti, R. dkk. Commissioning of the world's first compact pencil-beam scanning proton therapy system. (2017) doi: 10.1002/acm2.12225.
[19] Werner, C. J. MCNP User's Manual Code Version 6.2. *Los Alamos Natl. Lab.7*46 (2017).
[20] ICRP. Annals of the ICRP. *Ann. ICRP* **6**, 1 (2003).
[21] Fasihu, M. F. K., Harto, A. W., Triatmoko, I. M., Wijaya, G. S. & Sardjono, Y. Radiation Dose Optimization of Breast Cancer With Proton Therapy Method Using Particle and Heavy Ion Transport Code System. *J. Teknol. Reakt. Nukl. Tri Dasa Mega* **23**, 79 (2021).
[22] Anchineyan, P., Mani, G. K., Amalraj, J., Karthik, B. & Anbumani, S. Use of Flattening Filter - Free Photon Beams in Treating Medulloblastoma: A Dosimetric Evaluation. *ISRN Oncol.2***014**, 1–5 (2014).
[23] B, E. Tolerance of Normal Tissue to Therapeutic Radiation. *Reports Radiother. Oncol.1*, (2013).
[24] Sharyan, H. A., Allehyani, S. H. & Tolba, A. R. Dosimetric Comparison of 3DCRT Versus RapidArc in Terms of Iso - dose Distribution, Dose Volume Histogram (DVH) and Dosimetric Results for the PTV and Critical Organs for Glioblastoma (GBM). *Am. J. Med. Med. Sci.2***015**, 208–219 (2015).
[25] İbiş, K., Akbaş, U., Köksal, C. & Altun, M. Comparison of three - dimensional conformal radiation therapy, intensity - modulated radiation therapy, and volumetric - modulated arc therapy in glioblastoma multiforme radiation therapy with EORTC target delineation. *Turk Onkol. Derg.3***3**, 65–72 (2018).
[26] Carbonara, R., Di Rito, A., Monti, A., Rubini, G. & Sardaro, A. Proton versus Photon Radiotherapy for Pediatric Central Nervous System Malignancies: A Systematic Review and Meta - Analysis of Dosimetric Comparison Studies. *J. Oncol.2***019**, (2019).
[27] Helal, A., Mostafa, M. F., Elsaka, R. & Fadel, S.3DCRT for posterior fossa: Sparing of surrounding organs at risk. *Alexandria J. Med.5***0**, 311–316 (2014)
[28] Madkhali, A. M. Modelling Secondary Cancer Risk From Photon And Proton Therapy In Medulloblastoma. (Oxford University, 2018).